THE JOURNAL OF PHYSICAL CHEMISTRY C

ARTICLE

pubs.acs.org/JPCC

Lewis Acidity of Pt-Doped Buckybowls, Fullerenes, and Single-Walled Carbon Nanotubes

Charles See Yeung and Yan Alexander Wang*

Department of Chemistry, University of British Columbia, Vancouver, British Columbia V6T 1Z1, Canada

Supporting Information

ABSTRACT: The Lewis acidic character of alkyl- and arylplatinum complexes has been investigated within density functional theory with an emphasis on supramolecular structures (e.g., buckybowls, fullerenes, and nanotubes) doped with Pt atoms. By selective substitution of a single atom within a larger carbon framework with a Pt atom, the resulting species demonstrate a strong preference for interaction with small organic molecules, particularly polar substances via a Lewis acid/Lewis base complexation. Coordination with CO and maleic anhydride offers a gauge of comparing the Lewis acidity of these alkyl- and arylplatinum complexes. We have also examined the use of these organometallic species as catalysts for the Diels−Alder reaction and have found that curved π-conjugation and delocalization of electrons offer modest rate enhancements and improvements in selectivity. Preliminary results suggest that extended molecular architectures such as Pt-doped nanotubes may provide selectivities that differ from that of traditional Lewis acid catalysts.

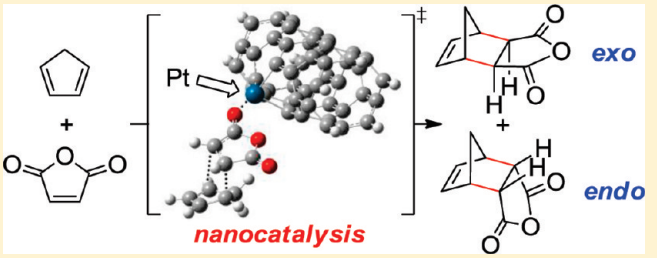

1. INTRODUCTION

The discovery of single-walled carbon nanotubes (SWCNTs) by Iijima in 1993[1] sparked a general interest in the investigation of the chemical and physical properties of this unique allotrope of carbon.[2] Through both experiment and theory, significant advancements in nanoscience have been made over the past 18 years, aimed at the development of SWCNTs for applications in molecular electronics,[3] sensory technology,[4,5] and catalysis,[6] among others.

SWCNTs are classified as metallic or semiconducting, depending on the diameter and chirality of the tube as prescribed by the wrapping vector (m,n).[7−10] While these macromolecules can be considered a seamless graphene cylinder constructed by rolling up a two-dimensional graphite layer, the curvature of the nanotube has a strong influence on electronic structure. Importantly, this leads to a pyramidalization of the C atoms, weakening the π-conjugation of the SWCNT. Each individual atom exhibits partial sp^3 hybridization, a net rehybridization of σ-, σ^*-, π-, and π^*-orbitals within the sidewall itself. Simplistically, this can be viewed as the partial incorporation of the atomic s orbitals into the atomic p_π orbitals.[7]

The quantification of curved π-conjugation of fullerenes and nanotubes can be achieved with the π-orbital axis vector (POAV) method of Haddon (Figure 1).[7,11] In this scheme, the pyramidalization angle (θ_p) is defined as

$$\theta_p = \theta_{\sigma\pi} - 90^\circ \quad (1)$$

where $\theta_{\sigma\pi}$ is the angle between the π-orbital and the σ-bond. For ethylene (C_2H_4), $\theta_p = 0^\circ$, meaning that the molecule is planar. In contrast, the sp^3-hybridized methane molecule exhibits a pyramidalization angle of $\theta_p = 19.5^\circ$. The icosahedral fullerene C_{60} displays $\theta_p = 11.6^\circ$, suggesting some deviation and planarity and, consequently, an increase in strain energy. Extended SWCNTs exhibit less pyramidalization, with $\theta_p = 6.0^\circ$. While there is a slight misalignment of the π-orbitals for adjacent C atoms within the nanotube structure, the bending typically results in less overall curvature than for fullerenes. As a result, SWCNTs are generally more inert than the corresponding fullerenes of similar diameters.[7,12]

The electronic properties of SWCNTs can be modified through functionalization[7] or doping.[7,13] Functionalization has been studied extensively, mainly taking advantage of the delocalized π-electron density along the backbone. For example, fluorination/nucleophilic substitution,[14] ozonolysis,[15] Diels−Alder cycloaddition,[16] osmylation,[17] hydroboration,[18] addition of carbenes[19] and nitrenes,[20] vinylcarbonylation via zwitterionic intermediates,[21] and radical alkylation[19,22] and arylation[23] strategies have been considered. Replacement of a C atom within the backbone with a heteroatom such as B and N has also been investigated by thermal treatment,[24] chemical vapor deposition,[25] laser ablation,[26] and the arc method.[27] Unfortunately, the concentration of doping atoms and their locations are difficult to control.[13] In light of this challenge, Srivastava et al. proposed the interaction between a free gas-phase neutral N atom and a vacancy in the C backbone of a SWCNT.[28] Later, work from

Received: August 27, 2010
Revised: February 25, 2011
Published: March 29, 2011

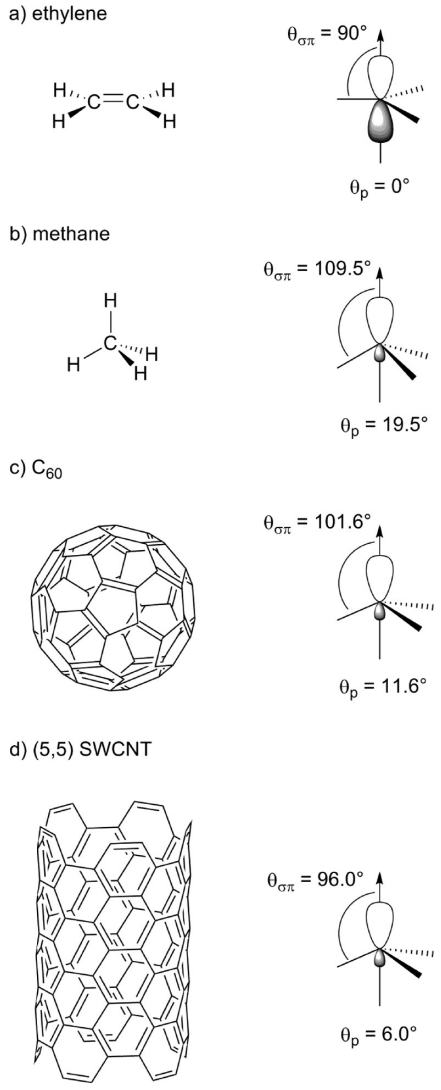

Figure 1. POAV analysis of curved π-conjugation in (a) ethylene, (b) methane, (c) C_{60}, and (d) a truncated (5,5) SWCNT.

our group suggested the use of NO as a N source, liberating a molecule of NO_2 as the byproduct.[29] A similar theoretical study was further conducted on the interaction with the transition metal Ni.[30] The direct incorporation of a transition metal atom, however, is yet to be achieved.[4,31]

We became interested in transition metal-doped nanotubes, specifically Pt-doped SWCNTs, due to the interesting geometric and electronic properties of this hypothetical material, as well as possible applications in the real world.[4,10,31] Notably, we have considered its application as a nanosensor by evaluating the adsorption of small gas molecules onto Pt centers localized on the sidewall of (5,5) SWCNTs. Our calculations predicted a strong, exothermic interaction between the adsorbate and the nanotube itself for a number of different species with varying polarities, including CO, NO, NH_3, N_2, H_2, C_2H_4, and C_2H_2.[4] From our earlier work[4] that had revealed a similarity between Pt-doped SWCNTs and $PtMe_3^+$, a strong Lewis acid,[32] we herein report a systematic study on the Lewis acidity of Pt-doped SWCNTs and other model alkyl- and arylplatinum complexes, including Pt-doped fullerenes. Their application to nanocatalysis, specifically in regards to the Diels–Alder reaction, will also be discussed.

2. THEORETICAL CALCULATIONS

A smaller model segment containing 30 C atoms and 10 capping H atoms ($C_{30}H_{10}$) was chosen to represent the (5,0) zigzag SWCNT. A single C atom in the middle of the segment was replaced with a Pt atom (Figure 2), yielding $C_{29}H_{10}Pt$ (**1a**). In addition, we also performed calculations on a larger system containing 50 C atoms and 10 capping H atoms ($C_{50}H_{10}$). An analogous Pt-doped model with formula $C_{49}H_{10}Pt$ (**1b**) was considered. Our previous work has shown that the termination of the nanotube segment with either H atoms or fullerene caps results in the same predicted geometries.[4,10,31]

Density functional theory (DFT) calculations were performed using the hybrid Hartree–Fock/DFT method B3LYP.[33] Relativistic effects (for the Pt atom) were incorporated using the relativistic effective core pseudopotential (ECP) of Hay and Wadt (LANL2).[34] Geometry optimization was first achieved with the smaller LANL2MB basis set and refined with the larger LANL2DZ basis set (Dunning/Huzinaga valence double-ζ for first row elements and Los Alamos ECP plus double-ζ for heavier elements)[35] with no restriction on symmetry. To validate these calculations, we also explored the larger LACVP* basis set (LANL2DZ with d polarization functions on all C and O atoms, i.e., 6-31G*).[36] By and large, the geometric and electronic structure as evaluated by partial charge and molecular orbital analyses did not reveal any significant discrepancies between the two sets of basis functions. Hereafter, we will mainly focus our discussion on the results based on the LANL2DZ basis set, unless specified otherwise.

The Hessian was calculated to verify the nature of all stationary points (i.e., local minima or transition states). Single-point calculations were conducted at the LANL2DZ level to obtain the frontier molecular orbitals (FMOs): the highest occupied molecular orbital (HOMO) and the lowest unoccupied molecular orbital (LUMO). Partial charges were evaluated by natural bond orbital (NBO) analysis using NBO 3.1[37] in the Gaussian 03 package.[38] The Gaussian 03 quantum chemical package was used for all calculations.[38] Both spin-restricted and spin-unrestricted optimizations yielded the same results for all ground-state complexes examined.[4,31]

To evaluate the Lewis acidity of **1**, a series of model systems were considered (Figure 3), including $PtMe_3^+$ (**2**), $PtPh_3^+$ (**3**), Pt-doped phenaline (**4**), Pt-doped sumanene (**5**), Pt-doped corannulene (**6**), and Pt-doped C_{24} fullerene (**7**). It should be noted that there are two distinct structural isomers of **7**, one in which the Pt atom substitutes a C atom at the junction between three pentagons (PPP, **7a**) and the other in which the Pt atom substitutes a C atom at the junction between a hexagon and two pentagons (HPP, **7b**). Each system was generated from the corresponding all-carbon analog, followed by Pt substitution and geometry optimization.

The adsorption of CO onto the Pt-doped SWCNT and model systems (Figures 2 and 3) was also examined. On the basis of our previous work regarding Pt-doped SWCNTs and model alkylplatinum complexes,[4,31] the adsorption of CO through the C atom is more energetically favorable. For simplicity, only the adsorption through the C atom was considered. The vibrational frequencies for the C≡O stretch were used as an indicator for the level of backdonation from the metal center to the ligand (vida infra).

The potential application of all alkyl- and arylplatinum complexes (**1**–**7**) as Lewis acids in catalysis was evaluated by two methods. First, the nuclear magnetic resonance (NMR) chemical shift (δ) of the olefinic H in the β position of maleic anhydride (**8**), an α,β-unsaturated carbonyl compound (Figure 4), was calculated and compared to traditional Lewis acids (i.e., $AlCl_3$,

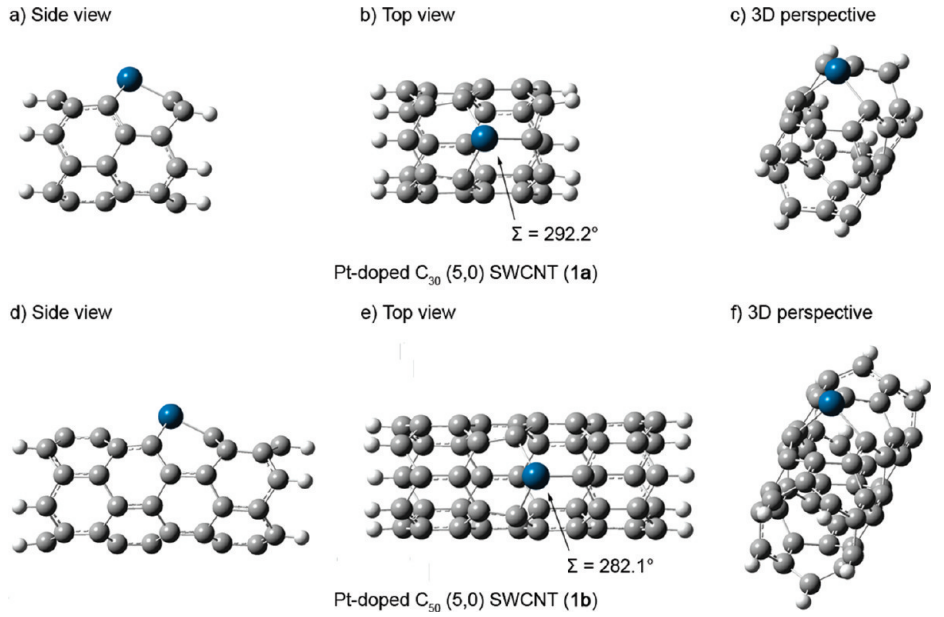

Figure 2. Optimized geometries of model Pt-doped (5,0) SWCNT segments (**1**).

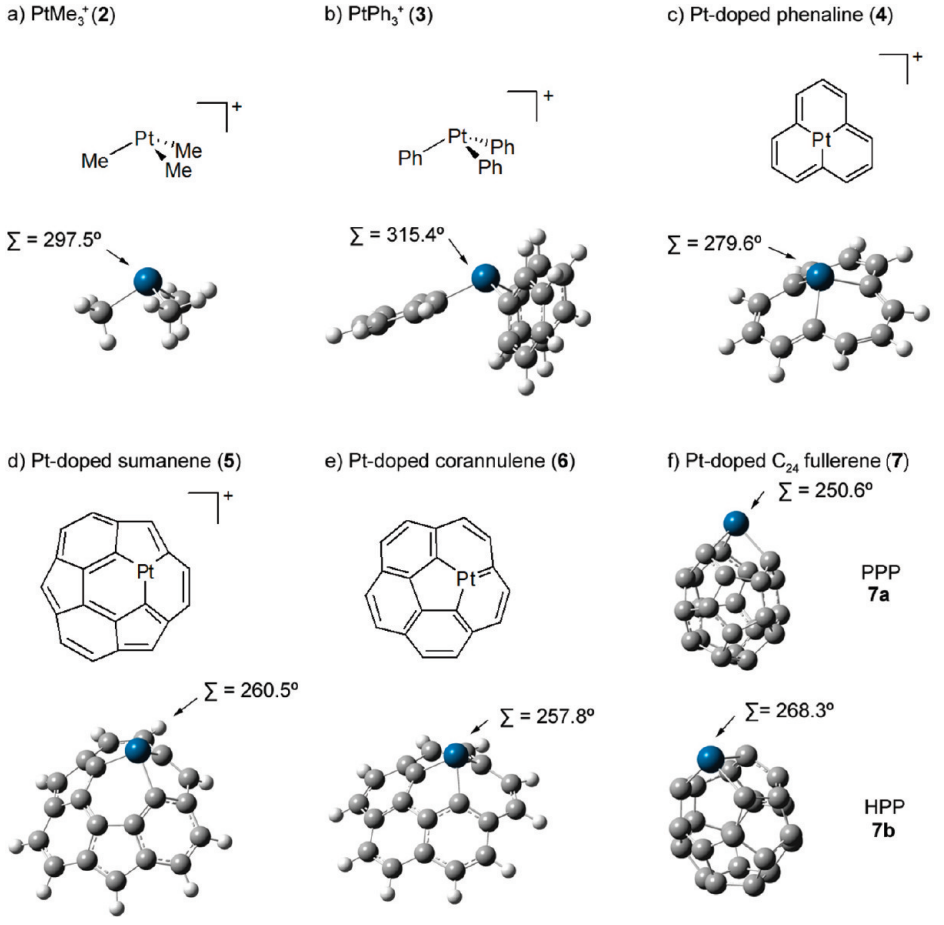

Figure 3. Optimized geometries of model alkyl- and arylplatinum complexes (**2**−**7**).

$AlMe_3$, BF_3, BCl_3, BBr_3, $SnCl_4$, and $TiCl_4$) as developed by Childs and co-workers.[39,40] As compared to the uncomplexed Lewis base, the presence of a Lewis acid is expected to result in a positive downfield shift due to an electron-withdrawing or deshielding effect. The chemical shift difference $\Delta\delta$ is thus a direct measure of Lewis acidity. Second, the rate enhancement of the Diels−Alder

dx.doi.org/10.1021/jp108174b |*J. Phys. Chem. C* 2011, 115, 7153–7163

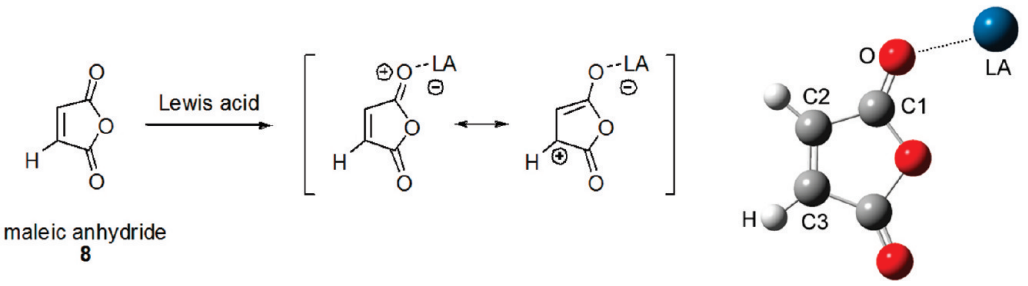

Figure 4. Chemical shift perturbation of β-H in maleic anhydride upon exposure to a Lewis acid (LA).

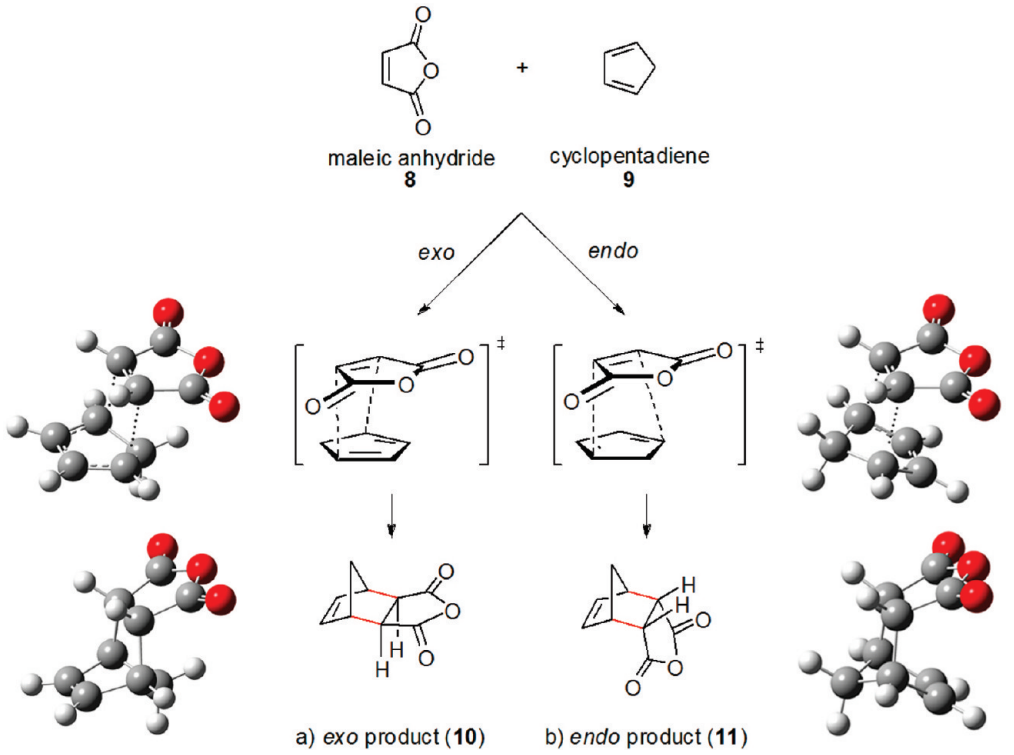

Figure 5. Diels–Alder cycloaddition between maleic anhydride (**8**) and cyclopentadiene (**9**) by (a) *exo* and (b) *endo* transition states.

reaction between maleic anhydride and cyclopentadiene (**9**) was evaluated (Figure 5). Both *exo* and *endo* transition states were considered. Previous work by other groups has suggested important solvent implications and other subtle effects,[41] which for simplicity were not considered in this study.

3. RESULTS AND DISCUSSION

3.1. Bare Alkyl- and Arylplatinum Complexes. We have recently reported a full account on truncated Pt-doped (5,5) SWCNTs and their ability to bind small gaseous molecules[4] and have identified simple alkylplatinum complexes (i.e., $PtMe_3^+$, **2**) as appropriate models to these macromolecular systems. In particular, the cationic $PtMe_3^+$ (**2**) was observed to bear the most similarity with the extended nanostructure among a series of alkylplatinum complexes considered in terms of geometry, localized charge, and ability to bind CO as a ligand.[31] The model systems chosen for this investigation also extend the analysis to include aromatic ligands ($PtPh_3^+$, **3**) and cyclic C frameworks (**4**–**6**). The buckybowl-type architectures **5** and **6**[42] are derived from smaller pieces of C_{60} fullerene, sumanene, and corannulene, respectively. The geometrically confined C_{24} skeleton (**7**) was also explored as a means of studying the direct effect of curvature and π-conjugation on the Lewis acidity of Pt-doped SWCNTs. In all scenarios, singlet ground states were probed by DFT with a single cationic charge as necessary (vida supra).

Bare Pt-doped (5,0) SWCNTs (**1**) exhibit a similar geometry to Pt-doped (5,5) SWCNTs in that the Pt atom protrudes to the exterior of the nanotube sidewall (Figure 2), likely because of the larger atomic radius of Pt and longer Pt–C bonds.[4,31] The three neighboring C atoms are arranged in a tripodal fashion around the pyramidalized Pt center, a significant deviation from planarity (Σ = 292.2° for **1a**, Σ = 282.1° for **1b**, cf. Σ = 360° for a planar hybridization scheme). Both Pt-doped C_{30} and C_{50} (5,0) SWCNT models (**1**) exhibited similar geometric and electronic properties. The simple alkylplatinum (**2**) and arylplatinum (**3**) both display less pyramidalization (Σ = 297.5° and 315.4°, respectively), which is expected because the C framework is not tied back in these scenarios. Surprisingly, the Pt-doped analog of phenaline (**4**), a segment of the idealized graphene

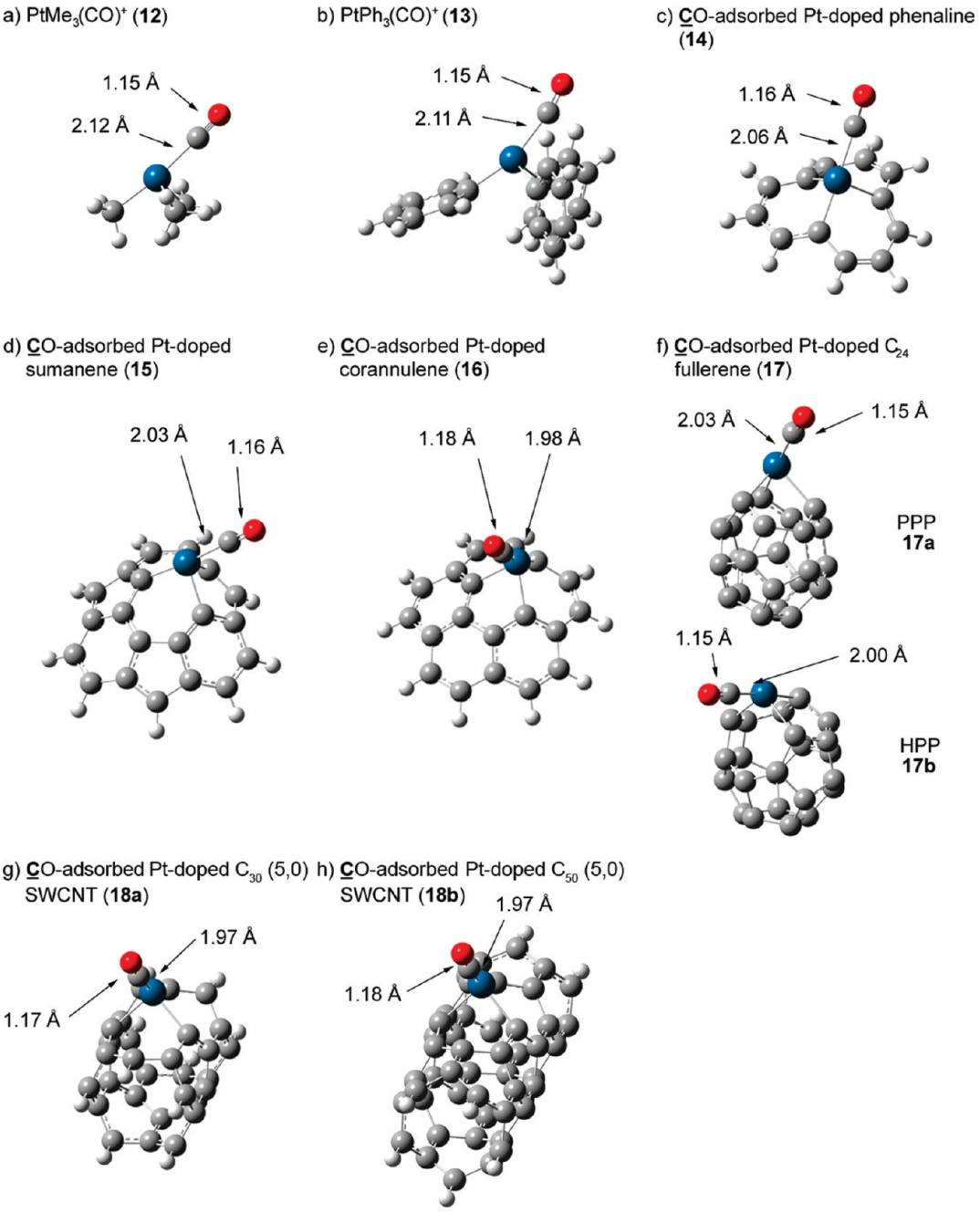

Figure 6. Optimized geometries of model CO-adsorbed model alkyl- and arylplatinum complexes. CO adsorption refers to binding through the C atom.

sheet, exhibit high levels of buckling ($\Sigma = 279.6°$). The fullerene model systems, Pt-doped sumanene (**5**), Pt-doped corannulene (**6**), and Pt-doped C_{24} (PPP and HPP isomers, **7**), are more highly pyramidalized than any of the other systems investigated, exceeding the hypothetical summation of angles predicted for three perfectly orthogonal ligands on a Pt center in an all *p*-orbital hybridization scheme ($\Sigma = 270°$). A brief analysis of the FMOs reveals a significant interaction between the metal d orbitals and the delocalized C framework, depending strongly on the curvature of the system investigated (see Figure 1S in the Supporting Information for details). In particular, the amount of electron density present on the Pt center appears quite diminished in Pt-doped fullerenes and SWCNTs.

3.2. Adsorption of Carbon Monoxide. The importance of CO as a ligand and adsorbate to transition metals (e.g., Pt) in both homogeneous[43] and heterogeneous[44] systems have been well explored. Pt-doped SWCNTs represent a unique niche in between the two extremes, possessing aspects of both the molecular and the supramolecular scales. We decided to examine the coordination of CO to alkyl- and arylplatinum complexes as a gauge of Lewis acidity. Because our previous work has showed that the adsorption of CO to Pt atoms occurs through the C atom preferentially,[4,31] we opted to limit our investigation to CO-adsorbed alkyl- and arylplatinum complexes (**12**−**18**, Figure 6). In the traditional sense, the binding of CO occurs via donation of σ-electrons from the C atom to the unoccupied metal d orbitals,

Table 1. Electronic Structural Data for Alkyl- and Arylplatinum Complexes and Their CO Adsorbates

Pt complex	Σ^a (deg)	q(Pt)^b	$E_{elec}{}^c$	ΔG^d	d(Pt−C)^e	d(C≡O)^e	$\nu_{C\equiv O}{}^f$	q(Pt/CO)^g	q(CO)^h
$PtMe_3^+$ (**2**)	297.5	0.77	−24.02	−8.25	2.116	1.156	2089.3	0.54	0.25
$PtPh_3^+$ (**3**)	315.4	0.77	−16.83	−0.46	2.113	1.160	2055.1	0.54	0.22
Pt-doped phenaline (**4**)	279.6	0.74	−28.58	−13.07	2.057	1.161	2050.3	0.40	0.23
Pt-doped sumanene (**5**)	260.5	0.77	−35.16	−19.67	2.025	1.163	2043.4	0.39	0.21
Pt-doped corannulene (**6**)	257.8	0.59	−34.30	−18.22	1.983	1.179	1949.4	0.26	0.08
Pt-doped C_{24} PPP isomer (**7a**)	250.6	0.69	−31.58	−16.74	2.027	1.167	2017.3	0.32	0.17
Pt-doped C_{24} HPP isomer (**7b**)	268.3	0.66	−32.71	−17.59	1.995	1.166	2026.4	0.30	0.22
Pt-doped C_{30} (5,0) SWCNT (**1a**)	292.2	0.53	−36.02	−20.31	1.971	1.179	1949.8	0.12	0.12
Pt-doped C_{50} (5,0) SWCNT (**1b**)^i	282.1	0.59	−34.33	−23.94	1.971	1.181	1934.0	0.13	0.09
	(284.0)	(0.44)	(−26.75)	(−16.51)	(1.982)	(1.154)	(2073.2)	(0.01)	(0.11)

[a] Sum of angles around Pt center (without adsorbate). [b] Partial charge on Pt atom (without adsorbate). [c] Electronic energy of stabilization (in kcal/mol) upon CO adsorption. [d] Free energy of stabilization (in kcal/mol) upon CO adsorption at 298 K. [e] Bond length (in Å) between atoms X and Y. [f] Vibration frequency (in cm^{-1}) of bound C≡O molecule (cf. 2028.8 cm^{-1} for unbound free CO). [g] Partial charge of Pt atom in CO-adsorbed Pt complex. [h] Partial charge on bound CO molecule. [i] Results with the LAC3VP* basis set are in parentheses.

stimulating the metal center to backdonate electrons to the π^*-orbital of the adsorbate. An increase in the electron density on the metal results in further reduction of the energy of the C≡O bond due to additional backbonding.[45] Hence, by analyzing the vibrational frequencies of CO molecules bound to alkyl- and arylplatinum complexes **1**−**7**, we can indirectly measure Lewis acidity, especially in relation to π-conjugation. Specifically, a lower C≡O stretching frequency implies lower Lewis acidity and vice versa. In all scenarios, the binding of CO and the formation of an alkyl- or arylplatinum−CO complex is expected to be energetically favorable.[4,31] In agreement with our previous work on Pt−CO interactions, simple alkyl- and arylplatinum complexes have a tendency to deplete electron density from the adsorbate (Table 1). Interestingly, while a Pt-doped (5,5) SWCNT model system exhibits net backdonation to the CO molecule, the Pt-doped (5,0) SWCNT model system demonstrates net donation of electron density from the CO molecule.

The trend of Lewis acidity suggested by adsorption of CO is as follows: Pt-doped (5,0) SWCNTs (**1**) ∼ Pt-doped corannulene (**6**) < Pt-doped C_{24} PPP isomer (**7a**) < Pt-doped C_{24} HPP isomer (**7b**) < Pt-doped sumanene (**5**) < Pt-doped phenaline (**4**) < $PtPh_3^+$ (**3**) < $PtMe_3^+$ (**2**).

It appears that Pt-doped (5,0) SWCNTs (**1**) are most similar to fullerene models, Pt-doped corannulene (**6**), and Pt-doped C_{24} (**7**), in their strong affinity for small gaseous molecules, even though the pyramidalization of the individual Pt atoms do not suggest such similarity (see Figures 2 and 3). In these cases, the electron delocalization within the extended C frameworks for both the nanotube and the fullerene models lessens the net positive charge buildup on the Pt nucleus, hence decreasing net Lewis acidity. The ability for backbonding, however, is increased. In addition, the presence of π-orbitals adjacent to the Pt atom is able to interact with the molecular orbitals of the adsorbate, increasing the energy released upon adsorption. Thus, a tight Pt−CO interaction (∼2.00 Å) is observed. The molecular orbitals of these model CO-adsorbed alkyl- and arylplatinum complexes highlight the varied levels of interaction between the adsorbate and the Pt nucleus (see Figure 2S in the Supporting Information for details).

Pt-doped phenaline (**4**) appears to be more Lewis acidic ($\nu_{C\equiv O}$ = 2050.3 cm^{-1}) than the other arylplatinum complexes (**1** and **5**−**7**). It should be noted that this arylplatinum complex, unlike the aforementioned fullerene and nanotube models, exhibits lower levels of π-curvature in the C backbone and increased levels of planarity. This suggests that distortion of adjacent π-orbitals imposed by supramolecular curvature decreases the effective Lewis acidity of doped transition metal nuclei. The bare $PtMe_3^+$ (**2**) and $PtPh_3^+$ (**3**) complexes exhibit the weakest interaction with CO molecules with d(Pt−C) ∼ 2.11 Å, in agreement with the observation that decreased π-curvature and π-conjugation lead to an increase in Lewis acidity and weaker backbonding. On the basis of this hypothesis, we would expect Pt-doped phenaline (**4**), $PtMe_3^+$ (**2**), and $PtPh_3^+$ (**3**) to be superior to arylplatinum complexes with higher π-curvature (**1** and **5**−**7**) in their ability to catalyze chemical reactions (vida infra).

3.3. Interaction with Maleic Anhydride (8). In 1982, Childs and co-workers suggested a general quantitative way of comparing Lewis acidity of different complexes.[39] By exposing an α,β-unsaturated carbonyl compound to different Lewis acids, the chemical shift δ of the olefinic H in the β position was observed to shift downfield (i.e., higher ppm). We chose to study maleic anhydride (**8**) and its interactions with traditional Lewis acids (i.e., $AlCl_3$, $AlMe_3$, BF_3, BCl_3, BBr_3, $SnCl_4$, and $TiCl_4$) as developed by Childs and co-workers (Figure 4).[39,40] As compared to the uncomplexed Lewis base, the presence of a Lewis acid is expected to result in a positive downfield shift due to an electron-withdrawing or deshielding effect.

Additionally, bond lengths were taken as indirect measures of Lewis acidity, since a more Lewis acidic species would result in a more significant weakening of the C1═O bond, strengthening of the C1−C2 bond and weakening of the C2═C3 bond (i.e., the bond between the α and β carbons). In agreement with this analysis, the coordination of **8** to a traditional Lewis acid or an alkyl- or arylplatinum complex generally results in a decreased C1−C2 bond length and increased C1═O and C2═C3 bond lengths (Table 2). This is because contribution from the resonance structure involving charge separation gains more weight as a result of Lewis acid/Lewis base pair formation. Accordingly, reactivity at C2 and C3 is presumed to increase as a result of this binding due to polarization of the previously symmetrical molecule. In addition, a decrease in the electron density is expected at C3, whereas an increase in the electron density is expected at the O atom (although this is complicated by the delocalization of charge onto the Lewis acid).

Our calculations confirmed that complexation between maleic anhydride and Lewis acids typically results in a downfield shift of

Table 2. Electronic Structural Data for Lewis Acid/Maleic Anhydride (8) Complexes

LA/**8** complex	d(C1═O)[a]	d(C1−C2)[a]	d(C2═C3)[a]	q(O)[b]	q(C3)[c]	δ(H)[d]	$\Delta\delta$(H)[e]
uncoordinated maleic anhydride (**8**)[f]	1.223 (1.198)	1.499 (1.491)	1.351 (1.335)	−0.496 (−0.500)	−0.250 (−0.276)	6.25 (6.08)	0.00 (0.00)
$PtMe_3^+$ (**2**)/**8**	1.248	1.488	1.354	−0.583	−0.215	7.02	0.77
$PtPh_3^+$ (**3**)/**8**	1.243	1.488	1.354	−0.557	−0.221	6.94	0.69
Pt-doped phenaline (**4**)/**8**	1.249	1.486	1.356	−0.584	−0.229	6.80	0.55
Pt-doped sumanene (**5**)/**8**	1.249	1.484	1.356	−0.577	−0.221	6.71	0.46
Pt-doped corannulene (**6**)/**8**	1.278	1.440	1.384	−0.643	−0.311	5.53	−0.72
Pt-doped C_{24} PPP isomer (**7a**)/**8**	1.254	1.472	1.363	−0.595	−0.266	6.30	0.05
Pt-doped C_{24} HPP isomer (**7b**)/**8**	1.245	1.479	1.359	−0.552	−0.250	6.39	0.14
Pt-doped C_{30} (5,0) SWCNT (**1a**)/**8**	1.265	1.451	1.376	−0.604	−0.297	5.63	−0.62
Pt-doped C_{50} (5,0) SWCNT (**1b**)/**8**[f]	1.276 (1.242)	1.441 (1.444)	1.385 (1.361)	−0.636 (−0.586)	−0.317 (−0.326)	5.62 (5.54)	−0.63 (−0.54)
$AlMe_3$/**8**	1.238	1.487	1.355	−0.597	−0.245	6.36	0.11
$AlCl_3$/**8**	1.245	1.490	1.353	−0.675	−0.225	6.60	0.35
BBr_3/**8**	1.256	1.486	1.354	−0.569	−0.234	6.38	0.12
BCl_3/**8**	1.254	1.489	1.353	−0.555	−0.233	6.40	0.15
BF_3/**8**	1.244	1.492	1.352	−0.561	−0.234	6.48	0.23
$SnCl_4$/**8**	1.241	1.492	1.352	−0.622	−0.233	6.46	0.20
$TiCl_4$/**8**	1.237	1.492	1.352	−0.508	−0.236	6.41	0.16

[a] Bond length (in Å) between atoms X and Y. [b] Partial charge on O atom. [c] Partial charge on C3 atom. [d] Chemical shift (in ppm) on H atom (referenced to tetramethylsilane). [e] Difference in chemical shift (in ppm) on H atom relative to uncoordinated maleic anhydride (**8**) (referenced to tetramethylsilane). [f] Results with the LAC3VP* basis set are in parentheses.

the β-H ^{1}H NMR signal (Table 2). Surprisingly, Pt-doped (5,0) SWCNT (**1**) and Pt-doped corannulene (**6**) result in a *decreased* chemical shift of the β-H, implying that the charge-separated resonance structure is less important in these two systems (Figure 4). This is most likely due to a larger steric hindrance toward the productive coordination of maleic anhydride to the Pt atom. Otherwise, the Lewis acidity of alkyl- and arylplatinum model complexes appears to affect the chemical shift to a much larger degree than traditional Lewis acids (by ca. 0.5 ppm difference), with the exception of the Pt-doped fullerenes (**7**). These data support that most of our Pt complexes are strong Lewis acids. Moreover, the trend of Lewis acidity suggested by chemical shift analysis is virtually identical to the conclusion based on the adsorption of CO.

By bond length analysis, in comparison to traditional Lewis acids, the alkyl- and arylplatinum complexes studied appear roughly equivalent in terms of Lewis acidity. Two noteworthy cases for discussion are the Pt-doped (5,0) SWCNT (**1**) and Pt-doped corannulene (**6**). Contrary to evaluation of Lewis acidity by the stretching frequency of a bound CO molecule, the coordination of maleic anhydride appears to be more strongly affected by the ligands on the Pt nucleus. For instance, complexation of **1** and **6** results in larger deviations than with the corresponding simple alkyl- and arylplatinum complexes, $PtMe_3^+$ (**2**) and $PtPh_3^+$ (**3**), respectively. This suggests that higher levels of π-curvature and increased ability to favor delocalization of the electron density facilitate binding of Lewis bases to Lewis acidic Pt centers. However, a more subtle interplay between steric and electronic factors is obviously present, since the same trends are not observed for the other Pt-doped buckybowls (**4** and **5**) and fullerenes (**7**). Distortion of the electron density on the LUMO of the maleic anhydride (**8**) is typically quite small (see Figure 3S in the Supporting Information for details). Significant interaction between the LUMO with the lobes on the model alkyl- and arylplatinum complexes can only be observed for Pt-doped corannulene (**6**). It is worth mentioning here that for the maleic anhydride (**8**), FMO analysis revealed significant differences between the electronic structures of the nanotube-adsorbate complex for the shorter C_{30} model **1a** (Figure 3S in the Supporting Information) and the longer C_{50} model **1b** (see Figure 4S in the Supporting Information for more details). This can be attributed to end effects and suggests that for more complex systems, the larger model more accurately describes the chemical reactivity.

3.4. Diels−Alder Reaction between Maleic Anhydride (8) and Cyclopentadiene (9). CO coordination and maleic anhydride complexation are both indirect measures of the strength of Lewis acidity of alkyl- and arylplatinum complexes as Lewis acids. The true test of Lewis acidity ought to be in the ability to activate an organic molecule for a chemical reaction. For the purposes of this study, we have chosen the Diels−Alder reaction between maleic anhydride (**8**) and cyclopentadiene (**9**). This reaction is termed a [4 + 2] cycloaddition of a diene (i.e., cyclopentadiene) and an alkene (i.e., maleic anhydride) to form a cyclohexene derivative with the key driving force being the formation of two new σ-bonds at the expense of two π-bonds. Concerning the reaction of maleic anhydride and cyclopentadiene, the presence of Lewis acid catalysts lowers the energy of the LUMO of the dienophile (i.e., the alkene) by binding to a Lewis basic site, hence favoring energetic overlap between the LUMO of the dienophile and the HOMO of the diene in a normal electron demand Diels−Alder reaction.[46]

Two diastereomers can be produced as a result of the Diels−Alder reaction, termed the *endo* and *exo* products (Figures 5 and 7). The *endo* product is kinetically favored, presumed to involve so-called *secondary orbital interactions* between the two unreactive C atoms on the diene and the π-orbitals of the neighboring C═O groups on the alkene.[46,47] In contrast, under thermodynamic control, the *exo* product is accessible, although typically requiring prolonged reaction time. The distribution of products resulting from the Diels−Alder reaction can depend on the choice of reaction conditions.

dx.doi.org/10.1021/jp108174b |*J. Phys. Chem. C* 2011, 115, 7153–7163

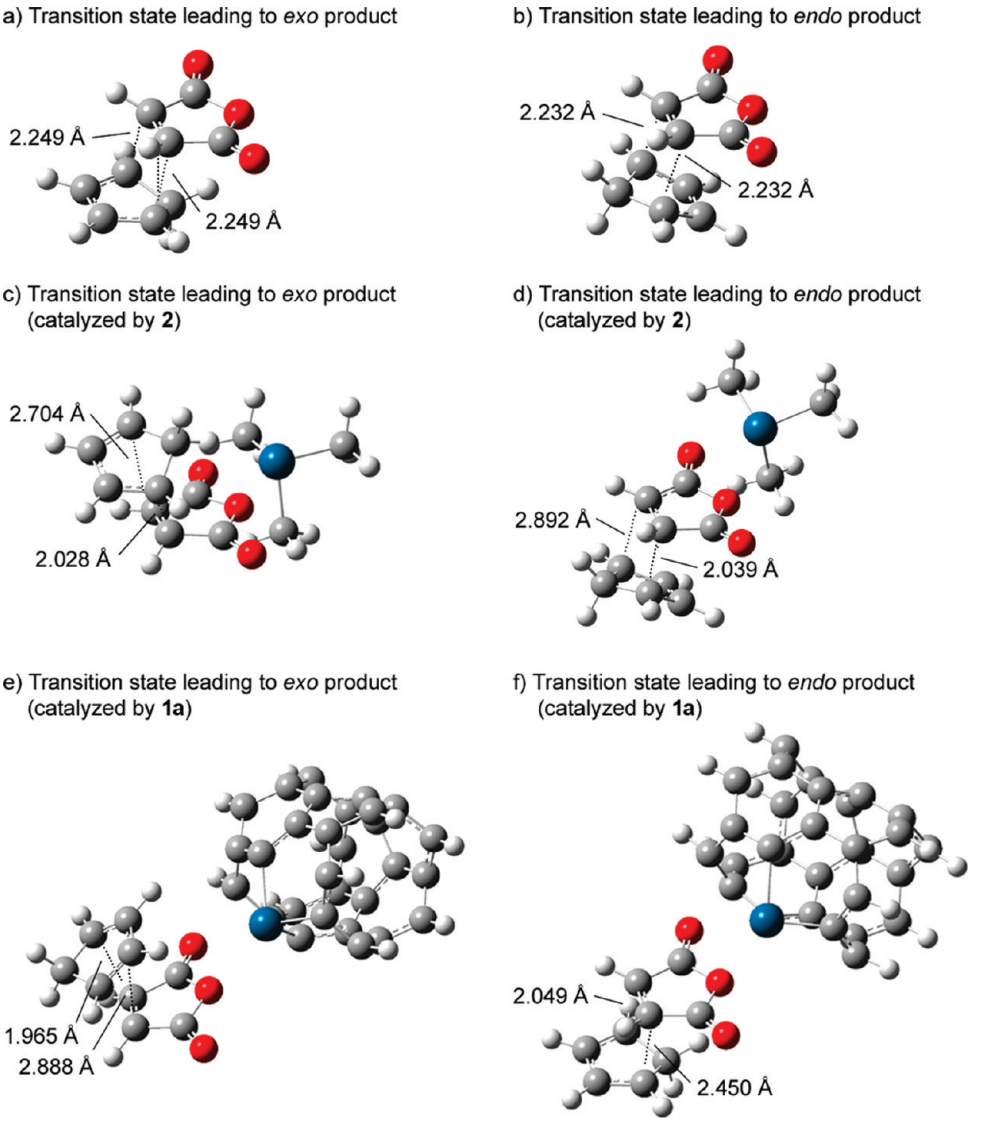

Figure 7. Transition states of the Diels–Alder reaction of maleic anhydride (**8**) and cyclopentadiene (**9**) as catalyzed by alkyl- and arylplatinum complexes.

Table 3. Free Energies and Rates of the Diels–Alder Reaction of Maleic Anhydride (8) and Cyclopentadiene (9) as Catalyzed by Alkyl- and Arylplatinum Complexes

catalyst	$\Delta G_{exo}^{\ddagger a}$	$\Delta G_{exo}{}^{b}$	$\Delta G_{endo}^{\ddagger c}$	$\Delta G_{endo}{}^{d}$	$\Delta\Delta G^{\ddagger e}$	$k_{endo}/k_{exo}{}^{f}$	$k_{cat}/k_{uncat}{}^{g}$
none	27.28	−3.83	26.67	−3.03	0.60	2.78	1.00
$PtMe_3^+$ (**2**)	15.85	−8.06	14.41	−9.54	1.44	11.43	1.27×10^3
$PtPh_3^+$ (**3**)	17.43	−8.19	16.82	−8.48	0.61	2.79	1.58×10^3
Pt-doped phenaline (**4**)	17.69	−8.15	16.67	−7.70	1.02	5.60	1.47×10^3
Pt-doped sumanene (**5**)	16.76	−8.57	16.19	−8.40	0.57	2.63	3.01×10^3
Pt-doped corannulene (**6**)	16.03	−13.26	15.30	−13.28	0.73	3.43	8.22×10^6
Pt-doped C_{24} PPP isomer (**7a**)	23.54	−4.04	22.68	−3.45	0.86	4.26	1.42
Pt-doped C_{24} HPP isomer (**7b**)	23.49	−4.47	22.49	−4.17	1.00	5.44	2.99
Pt-doped C_{30} (5,0) SWCNT (**1a**)	30.23	2.47	30.11	−3.47	0.12	1.23	0.55
Pt-doped C_{50} (5,0) SWCNT (**1b**)	30.97	6.36	31.89	6.52	−0.91	0.21	1.6×10^{-3}

[a] Free energy (in kcal/mol) required to reach transition state leading to *exo* product at 298 K. [b] Free energy change (in kcal/mol) to *exo* product in at 298 K. [c] Free energy (in kcal/mol) required to reach transition state leading to *endo* product at 298 K. [d] Free energy change (in kcal/mol) to *endo* product at 298 K. [e] Difference in free energy changes (in kcal/mol) required to reach transition states leading to *endo* and *exo* products at 298 K. [f] Relative rate leading to *endo* product versus *exo* product. [g] Relative rate of catalyzed Diels–Alder reaction versus uncatalyzed Diels–Alder reaction.

dx.doi.org/10.1021/jp108174b |*J. Phys. Chem. C* 2011, 115, 7153–7163

On the basis of our previous work, alkyl- and arylplatinum complexes (**1**−**7**), particularly Pt-doped nanotubes (**1**), are excellent Lewis acids.[31] We thus sought to evaluate the ability of such organometallic complexes to act as catalysts for the Diels−Alder reaction. While $PtMe_3^+$ has potential as a catalyst,[32] the use of Pt-doped supramolecules, such as buckybowls, fullerenes, and nanotubes, has not yet been realized. We explored the possibility of both *exo* and *endo* transition states in these catalytic systems and found a similarity with previous studies of the Diels−Alder reaction, suggesting a concerted but asynchronous transition state (Figures 5 and 7).[41,48]

The application of alkyl- and arylplatinum complexes as catalysts for the Diels−Alder reaction of maleic anhydride and cyclopentadiene generally results in an enhancement of reaction rate (Table 3). Interestingly, Pt-doped fullerene (**7**) demonstrates only an approximate 3-fold rate increase, while systems displaying less ability to delocalize the electron density yield greater enhancements (up to 10^7-fold). The application of a Pt-doped nanotube (**1a**) as Lewis acid catalyst actually results in a *decreased* reaction rate. With the larger Pt-doped C_{50} (5,0) SWCNT (**1b**), a similar qualitative trend was observed. Careful examination of the geometric structures (Figure 7) revealed that ligands on Pt centers with extended C frameworks generally give transition states that are more synchronous in character in comparison to the highly reactive $PtMe_3^+$ (**2**) and $PtPh_3^+$ (**3**). Thus, it seems that the polarization of the alkene (i.e., formation of the charge-separated species) appears to have the largest influence on catalyzing the [4 + 2] cycloaddition of a pair of diene and dienophile. The reason behind such an enhanced reactivity, however, is not clear since the reaction that we are studying involves two nonpolar starting materials (i.e., maleic anhydride and cyclopentadiene). In contrast, pyramidalization of the C framework appears to have relatively little impact on the effectiveness of the proposed catalysis.

Assuming kinetic control of the Diels−Alder reaction, in regard to the *endo* and *exo* distribution of products, it appears that the systems with higher levels of delocalization of the electron density in the catalyst give *lower* preference for the *endo* product. The system that gives one of the highest increases in rate ($PtMe_3^+$) also has the highest selectivity for the *endo* product. Virtually in no cases is the *exo* product favored over the *endo* product. Interestingly, with the extended Pt-doped SWCNTs (i.e., **1a** and **1b**), the chemical reactivity begins to favor the thermodynamic *exo* product, highlighting the potential of nanocatalysis to provide complementary selectivities and reactivities to traditional catalyst systems. This result is remarkable considering the similar geometric and electronic properties between the Pt-doped SWCNTs and other Pt-doped buckybowls and fullerenes (**4**−**7**).[49] Overall, it appears that decreased steric hindrance is ideal for promoting *endo* diastereoselectivity in the Diels−Alder reaction, whereas increased steric hindrance favors *exo* product formation. The generality of this statement, however, requires further investigation since we have chosen a *finite* model of a SWCNT with H capping atoms to examine the feasibility of catalysis. Moreover, the interaction between two metal centers in close proximity of each other as dopant atoms in an extended carbon framework or perhaps even through different SWCNTs with varied radii and chirality may play important roles in both the efficiency and the selectivity in catalysis.

Overall, the additional π-delocalization of electrons in Pt-doped supramolecular frameworks (e.g., buckybowls, fullerenes, and nanotubes) appears to offer less useful rate enhancements and selectivities in comparison with the readily available simple $PtMe_3^+$ system. However, the synthesis of Pt-doped fullerenes and nanotubes for use as catalysts remains an important challenge because of the potential to use the supramolecular C framework as a means of imparting additional *stability* to the otherwise highly active metal centers. This may have important implications in achieving effective heterogeneous Lewis acid catalysis,[4,31] in which immobilization of reactive Lewis acids is of particular interest and recovery and reuse of precious metals are also of concern.

4. CONCLUSION

We have evaluated the Lewis acidic character of alkyl- and arylplatinum complexes, including the supramolecular Pt-doped buckybowls, fullerenes, and nanotubes, via analysis of CO and maleic anhydride complexation, as well as potential utility as catalysts for the Diels−Alder reaction. On the basis of our investigation, it appears that there is no clear relationship between π-delocalization of electrons and Lewis acidity. Furthermore, curved π-conjugation is not a suitable predictor for ability of an alkyl- or arylplatinum complexes to bind small molecules such as CO and maleic anhydride. In terms of catalysis, the presence of C frameworks in supramolecular structures acting as ligands on Pt centers offers modest improvements in reaction rate and selectivity within the context of the Diels−Alder reaction, although still inferior in comparison to the simpler $PtMe_3^+$ system. Preliminary results suggest that Pt-doped SWCNTs may offer opportunities to achieve complementary selectivities in comparison to traditional Lewis acid catalysts. Additionally, the more complex buckybowls, fullerenes, and nanotubes containing a dopant Pt atom may impart additional stability to these otherwise highly reactive and unstable catalytic manifolds. Our work here should provide motivation for experimentalists to further pursue synthesis of these as of yet elusive Pt-doped supramolecular architectures.

■ ASSOCIATED CONTENT

Supporting Information. Molecular orbitals, optimized geometries (in Cartesian coordinates), and full citation for ref 38. This material is available free of charge via the Internet at http://pubs.acs.org.

■ AUTHOR INFORMATION

Corresponding Author
*E-mail: yawang@chem.ubc.ca.

■ ACKNOWLEDGMENT

The Natural Sciences and Engineering Research Council (NSERC) of Canada is gratefully acknowledged for financial support. WestGrid and C-HORSE provided computational resources for this study. C.S.Y. thanks NSERC for an Undergraduate Student Research Award.

■ REFERENCES

(1) Iijima, S.; Ichihashi, T. *Nature* **1993**, *363*, 603.
(2) (a) Tasis, D.; Tagmatarchis, N.; Bianco, A.; Prato, M. *Chem. Rev.* **2006**, *106*, 1105. (b) Ajayan, P. M. *Chem. Rev.* **1999**, *99*, 1787.
(3) (a) Avouris, P. *Acc. Chem. Res.* **2002**, *35*, 1026. (b) Robertson, N.; McGowan, C. A. *Chem. Soc. Rev.* **2003**, *32*, 96. (c) Chen, Z.; Appenzeller, J.;

Lin, Y.-M.; Sippel-Oakley, J.; Rinzler, A. G.; Tang, J.; Wind, S. J.; Solomon, P. M.; Avouris, P. *Science* **2006**, *311*, 1735. (d) Byon, H. R.; Choi, H. C. *J. Am. Chem. Soc.* **2006**, *128*, 2188.

(4) Yeung, C. S.; Liu, L. V.; Wang, Y. A. *J. Phys. Chem. C* **2008**, *112*, 7401.

(5) (a) Byon, H. R.; Choi, H. C. *J. Am. Chem. Soc.* **2006**, *128*, 2188. (b) Kose, M. E.; Harruff, B. A.; Lin, Y.; Veca, L. M.; Lu, F.; Sun, Y.-P. *J. Phys. Chem. B* **2006**, *110*, 14032. (c) Jeng, E. S.; Moll, A. E.; Roy, A. C.; Gastala, J. B.; Strano, M. S. *Nano Lett.* **2006**, *6*, 371. (d) Liu, J.; Tian, S.; Knoll, W. *Langmuir* **2005**, *21*, 5596. (e) Goldoni, A.; Larciprete, R.; Petaccia, L.; Lizzit, S. *J. Am. Chem. Soc.* **2003**, *125*, 11329.

(6) Serp, P.; Corrias, M.; Kalck, P. *Appl. Catal., A* **2003**, *253*, 337.

(7) Lu, X.; Chen, Z. *Chem. Rev.* **2005**, *105*, 3643.

(8) (a) Yeung, C. S.; Tian, W. Q.; Liu, L. V.; Wang, Y. A. *J. Comput. Theor. Nanosci.* **2009**, *6*, 1213. (b) Tian, W. Q.; Liu, L. V.; Chen, Y. K.; Wang, Y. A. Electronic Structure and Reactivities of Perfect, Defected, and Doped Single-Walled Carbon Nanotubes. *Trends in Computational Nanomechanics: Transcending Length and Time Scales*; Springer: Dordrecht, 2010; Chapter 16.

(9) (a) Hamada, N.; Sawada, S.-I.; Oshiyama, A. *Phys. Rev. Lett.* **1992**, *58*, 1579. (b) Dresselhaus, M. S.; Dresselhaus, G.; Eklund, P. C. *Science of Fullerenes and Carbon Nanotubes*; Academic Press Inc.: San Diego, 1995; Chapter 19.

(10) Tian, W. Q.; Liu, L. V.; Wang, Y. A. *Phys. Chem. Chem. Phys.* **2006**, *8*, 3528.

(11) (a) Haddon, R. C.; Scott, L. T. *Pure Appl. Chem.* **1986**, *58*, 137. (b) Haddon, R. C. *Science* **1993**, *261*, 1545.

(12) Chen, Z.; Thiel, W.; Hirsch, A. *ChemPhysChem* **2003**, *4*, 93.

(13) Terrones, M.; Jorio, A.; Endo, M.; Rao, A. M.; Kim, Y. A.; Hayashi, T.; Terrones, H.; Charlier, J.-C.; Dresselhaus, G.; Dresselhaus, M. S. *Mater. Today* **2004**, *7*, 30.

(14) (a) Stevens, J. L.; Huang, A. Y.; Peng, H.; Chiang, I. W.; Khabashesku, V. N.; Margrave, J. L. *Nano Lett.* **2003**, *3*, 331. (b) Saini, R. K.; Chiang, I. W.; Peng, H.; Smalley, R. E.; Billups, W. E.; Hauge, R. H.; Margrave, J. L. *J. Am. Chem. Soc.* **2003**, *125*, 3617. (c) Mickelson, E. T.; Huffman, C. B.; Rinzler, A. G.; Smalley, R. E.; Hauge, R. H.; Margrave, J. L. *Chem. Phys. Lett.* **1998**, *296*, 188.

(15) (a) Banerjee, S.; Wong, S. S. *J. Phys. Chem. B* **2002**, *106*, 12144. (b) Lu, X.; Zhang, L.; Xu, X.; Wang, N.; Zhang, Q. *J. Phys. Chem. B* **2002**, *106*, 2136.

(16) (a) Delgado, J. L.; de la Cruz, P.; Langa, F.; Urbina, A.; Casado, J.; Navarrete, J. T. L. *Chem. Commun.* **2004**, 1734. (b) Lu, X.; Tian, F.; Wang, N.; Zhang, Q. *Org. Lett.* **2002**, *4*, 4313.

(17) Lu, X.; Tian, F.; Feng, Y.; Xu, X.; Wang, N.; Zhang, Q. *Nano Lett.* **2002**, *2*, 1325.

(18) Long, L.; Lu, X.; Tian, F.; Zhang, Q. *J. Org. Chem.* **2003**, *68*, 4495.

(19) Holzinger, M.; Vostrowsky, O.; Hirsch, A.; Hennrich, F.; Kappes, M.; Weiss, R.; Jellen, F. *Angew. Chem., Int. Ed.* **2001**, *40*, 4002.

(20) Holzinger, M.; Abraham, J.; Whelan, P.; Graupner, R.; Ley, L.; Hennrich, F.; Kappes, M.; Hirsch, A. *J. Am. Chem. Soc.* **2003**, *125*, 8566.

(21) (a) Zhang, W.; Sprafke, J. K.; Ma, M.; Tsui, E. Y.; Sydlik, S. A.; Rutledge, G. C.; Swager, T. M. *J. Am. Chem. Soc.* **2009**, *131*, 8446. (b) Zhang, W.; Swager, T. M. *J. Am. Chem. Soc.* **2007**, *129*, 7714.

(22) Peng, H.; Alemany, L. B.; Margrave, J. L.; Khabashesku, V. N. *J. Am. Chem. Soc.* **2003**, *125*, 15174.

(23) Bahr, J. L.; Yang, J.; Kosynkin, D. V.; Bronikowski, M. J.; Smalley, R. E.; Tour, J. M. *J. Am. Chem. Soc.* **2001**, *123*, 6536.

(24) Golberg, D.; Bando, Y.; Han, W.; Kurashima, K.; Sato, T. *Chem. Phys. Lett.* **1999**, *308*, 337.

(25) Sung, S. L.; Tsai, S. H.; Tseng, C. H.; Chiang, F. K.; Liu, X. W.; Shih, H. C. *Appl. Phys. Lett.* **1999**, *74*, 197.

(26) Gai, P. L.; Stephan, O.; McGuire, K.; Rao, A. M.; Dresselhaus, M. S.; Dresselhaus, G.; Colliex, C. *J. Mater. Chem.* **2004**, *14*, 669.

(27) Glerup, M.; Steinmetz, J.; Samaille, D.; Stéphan, O.; Enouz, S.; Loiseau, A.; Roth, S.; Bernier, P. *Chem. Phys. Lett.* **2004**, *387*, 193.

(28) Srivastava, D.; Menon, M.; Daraio, C.; Jin, S.; Sadanadan, B.; Rao, A. M. *Phys. Rev. B* **2004**, *69*, 153414.

(29) Liu, L. V.; Tian, W. Q.; Wang, Y. A. *J. Phys. Chem. B* **2006**, *110*, 1999.

(30) Yang, S. H.; Shin, W. H.; Lee, J. W.; Kim, S. Y.; Woo, S. I.; Kang, J. K. *J. Phys. Chem. B* **2006**, *110*, 13941.

(31) Yeung, C. S.; Liu, L. V.; Wang, Y. A. *J. Comput. Theor. Nanosci.* **2007**, *4*, 1108.

(32) (a) Hsieh, V.; de Crisci, A. G.; Lough, A. J.; Fekl, U. *Organometallics* **2007**, *26*, 938. (b) Procelewska, J.; Zahl, A.; Liehr, G.; van Eldik, R.; Smythe, N. A.; Williams, B. S.; Goldberg, K. I. *Inorg. Chem.* **2005**, *44*, 7732.

(33) (a) Becke, A. D. *J. Chem. Phys.* **1999**, *98*, 5648. (b) Lee, C.; Yang, W.; Parr, R. G. *Phys. Rev. B* **1988**, *37*, 785.

(34) Hay, P. J.; Wadt, W. R. *J. Chem. Phys.* **1985**, *82*, 299.

(35) Dunning, T. H.; Hay, P. J. *Modern Theoretical Chemistry*; Plenum: New York, 1976; Vol. 3.

(36) (a) Petersson, G. A.; Bennett, A.; Tensfeldt, T. G.; Al-Laham, M. A.; Shirley, W. A.; Mantzaris, J. *J. Chem. Phys.* **1988**, *89*, 2193–2218. (b) Petersson, G. A.; Al-Laham, M. A. *J. Chem. Phys.* **1991**, *94*, 6081–6090.

(37) (a) Reed, A. E.; Curtiss, L. A.; Weinhold, F. *Chem. Rev.* **1988**, *88*, 899. (b) Glendening, E. D.; Carpenter, A. E.; Weinhold, F. *NBO*, Version 3.1, 1995.

(38) Frisch, M. J.; Trucks, G. W.; Schlegel, H. B.; Scuseria, G. E.; Robb, M. A.; Cheeseman, J. R.; Montgomery, J. A., Jr.; Vreven, T.; Kudin, K. N.; Burant, J. C.; Millam, J. M.; Iyengar, S. S.; Tomasi, J.; Barone, V.; Mennucci, B.; Cossi, M.; Scalmani, G.; Rega, N.; Petersson, G. A.; Nakatsuji, H.; Hada, M.; Ehara, M.; Toyota, K.; Fukuda, R.; Hasegawa, J.; Ishida, M.; Nakajima, T.; Honda, Y.; Kitao, O.; Nakai, H.; Klene, M.; Li, X.; Knox, J. E.; Hratchian, H. P.; Cross, J. B.; Bakken, V.; Adamo, C.; Jaramillo, J.; Gomperts, R.; Stratmann, R. E.; Yazyev, O.; Austin, A. J.; Cammi, R.; Pomelli, C.; Ochterski, J. W.; Ayala, P. Y.; Morokuma, K.; Voth, G. A.; Salvador, P.; Dannenberg, J. J.; Zakrzewski, V. G.; Dapprich, S.; Daniels, A. D.; Strain, M. C.; Farkas, O.; Malick, D. K.; Rabuck, A. D.; Raghavachari, K.; Foresman, J. B.; Ortiz, J. V.; Cui, Q.; Baboul, A. G.; Clifford, S.; Cioslowski, J.; Stefanov, B. B.; Liu, G.; Liashenko, A.; Piskorz, P.; Komaromi, I.; Martin, R. L.; Fox, D. J.; Keith, T.; Al-Laham, M. A.; Peng, C. Y.; Nanayakkara, A.; Challacombe, M.; Gill, P. M. W.; Johnson, B.; Chen, W.; Wong, M. W.; Gonzalez, C.; Pople, J. A. *Gaussian 03*, revision B.05; Gaussian, Inc.: Wallingford, CT, 2003.

(39) Childs, R. F.; Mulholland, D. L.; Nixon, A. *Can. J. Chem.* **1982**, *60*, 801.

(40) Laszlo, P.; Teston, M. *J. Am. Chem. Soc.* **1990**, *112*, 8750.

(41) (a) DeChancie, J.; Acevedo, O.; Evanseck, J. D. *J. Am. Chem. Soc.* **2004**, *126*, 6043. (b) Acevedo, O.; Evanseck, J. D. *Org. Lett.* **2003**, *5*, 649. (c) Fu, Y.-S.; Tsai, S.-C.; Huang, C.-H.; Yen, S.-Y.; Hu, W.-P.; Yu, S. J. *J. Org. Chem.* **2003**, *68*, 3068. (d) Ruano, J. L. G.; Clemente, F. R.; Gutiérrez, L. G.; Gordillo, R.; Castro, A. M. M.; Ramos, J. R. *J. Org. Chem.* **2002**, *67*, 2926. (e) Brunkan, N. M.; Gagné, M. R. *Organometallics* **2002**, *21*, 1576. (f) Pignat, K.; Vallotto, J.; Pinna, F.; Strukul, G. *Organometallics* **2000**, *19*, 5160. (g) Birney, D. M.; Houk, K. N. *J. Am. Chem. Soc.* **1990**, *112*, 4127.

(42) (a) Wu, Y.-T.; Siegel, J. S. *Chem. Rev.* **2006**, *106*, 4843. (b) Tsefrikas, V. M.; Scott, L. T. *Chem. Rev.* **2006**, *106*, 4868.

(43) (a) Mastrorilli, P.; Nobile, C. F.; Suranna, G. P.; Fanizzi, F. P.; Ciccarella, G.; Englert, U.; Li, Q. *Eur. J. Inorg. Chem.* **2004**, 1234. (b) Houlis, J. F.; Roddick, D. M. *J. Am. Chem. Soc.* **1998**, *120*, 11020. (c) Puga, J.; Patrini, R.; Sanchez, K. M.; Gates, B. C. *Inorg. Chem.* **1991**, *30*, 2479.

(44) Orita, H.; Itoh, N.; Inada, Y. *Chem. Phys. Lett.* **2004**, *384*, 271.

(45) (a) Blyholder, G. *J. Phys. Chem.* **1964**, *68*, 2772. (b) Housecroft, C. E.; Sharpe, A. G. *Inorganic Chemistry*, 1st ed.; Pearson Education Ltd.: Essex, England, 2001; Chapter 23. (c) Spessard, G. O.; Miessler, G. L. *Organometallic Chemistry*, 1st ed.; Prentice-Hall, Inc.: Upper Saddle River, NJ, 1996; Chapter 4.

(46) Kürti, L.; Czakó, B. *Strategic Applications of Named Reactions in Organic Synthesis*; Elsevier Academic Press: Burlington, MA, 2005; p 140.

(47) García, J. I.; Mayoral, J. A.; Salvatella, L. *Acc. Chem. Res.* **2000**, *33*, 658–664.
(48) Sun, H.; Zhang, D.; Ma, C.; Liu, C. *Int. J. Quantum Chem.* **2007**, *107*, 1875.
(49) For a Lewis acid-catalyzed *exo*-selective Diels–Alder reaction with a sterically bulky aluminum complex catalyst, see the following: (a) Maruoka, K.; Imoto, H.; Yamamoto, Y. *J. Am. Chem. Soc.* **1994**, *116*, 12115. For other examples, see the following: (b) Boren, B.; Hirschi, J. S.; Reibenspies, J. H.; Tallant, M. D.; Singleton, D. A.; Sulikowski, G. A. *J. Org. Chem.* **2003**, *68*, 8991. (c) Ward, D. E.; Gai, Y. *Tetrahedron Lett.* **1992**, *33*, 1851.